JOURNAL OF BACTERIOLOGY, Jan. 1986, p. 244–251
0021-9193/86/010244-08$02.00/0

Vol. 165, No. 1

Synthesis of a Functional F_0 Sector of the *Escherichia coli* H^+-ATPase Does Not Require Synthesis of the Alpha or Beta Subunits of F_1

ROBERT H. FILLINGAME,* BRUCE PORTER, JOE HERMOLIN, AND LAURA K. WHITE

Department of Physiological Chemistry, University of Wisconsin, Madison, Wisconsin 53706

Received 29 July 1985/Accepted 5 October 1985

The *uncB*, *E*, *F*, and *H* genes of the *Escherichia coli unc* operon were cloned behind the *lac* promoter of plasmid pUC9, generating plasmid pBP101. These *unc* loci code, respectively, for the χ, ω, and ψ subunits of the F_0 sector and the δ subunit of the F_1 sector of the H^+-ATP synthase complex. Induction of expression of the four *unc* genes by the addition of isopropyl-β-D-thiogalactoside resulted in inhibition of growth. During isopropyl-β-D-thiogalactoside induction, the three subunits of F_0 were integrated into the cytoplasmic membrane with a resultant increase in H^+ permeability. A functional F_0 was formed from plasmid pBP101 in a genetic background lacking all eight of the *unc* structural genes coding the F_1F_0 complex. In the *unc* deletion background, a reasonable correlation was observed between the amount of F_0 incorporated into the membrane and the function measured, i.e., high-affinity binding of F_1 and rate of F_0-mediated H^+ translocation. This correlation indicates that most or all of the F_0 assembled in the membrane is active. Although the F_0 assembled under these conditions binds F_1, only partial restoration of NADH-dependent or ATP-dependent quenching of quinacrine fluorescence was observed with these membranes. Proteolysis of a fraction of the ψ subunit may account for this partial deficiency. The experiments described demonstrate that a functional F_0 can be assembled in vivo in *E. coli* strains lacking genes for the α, β, γ, and ε subunits of F_1.

The eight subunits of the H^+-ATPase complex of *Escherichia coli* are coded by the genes of the *unc* operon (11, 32). The *unc* genes are transcribed in the order *I*, *B*, *E*, *F*, *H*, *A*, *G*, *D*, *C*. The *B*, *E*, and *F* genes code for the three subunits of the H^+-translocating sector of the complex (F_0), subunits which we refer to as χ, ω, and ψ, respectively (4). These subunits are found in a ratio of 1:10:2 in the purified H^+-ATPase complex (7). The *H*, *A*, *G*, *D*, and *C* genes code for the five subunits of the extrinsic ATPase sector of the complex (F_1), coding, respectively, the δ, α, γ, β, and ε subunits. These subunits are found in a ratio of 1:3:1:3:1 in the purified F_1 or F_1F_0 complex (7). The *uncI* gene appears to be unimportant in expression of a functional complex (12). The unusual variance in ratio of subunits in the final complex raises the interesting question of how assembly of the complex is regulated from the single gene for each subunit in the *unc* operon. The first clear indication that the regulation of assembly would be complex came from the observation that insertion of bacteriophage Mu in genes distal to the genes encoding F_0 prevented formation of a functional F_0 (14). Subsequently, membranes from several *uncA* and *uncD* mutants were shown to lack F_0 activity, and the lack of activity was correlated with the apparent lack of incorporation of the *uncF* gene product into the membrane (2). Based upon these observations, Cox et al. (2) proposed an assembly model for F_1F_0 which required that the α and β subunits be present for insertion of the *uncF* protein (ψ subunit). Klionsky et al. (20) also concluded that expression of *uncA* and *uncD* was necessary for formation of a functional F_0, although in their studies, which utilized plasmids carrying different regions of the *unc* operon, the *uncF* protein was incorporated into the minicell membrane in the absence of the *uncA* (α) and *uncB* (β) genes. Previously, we presented evidence that a functional F_0 could be formed in the absence of the coordinated synthesis of F_1 subunits, but these experiments left open the possibility that F_1 subunits might be required catalytically in the process (5). Here we extend the findings from that preliminary report and show that a functional F_0 is formed from a plasmid carrying only the *B*, *E*, *F*, and *H* genes in a cell lacking any α or β subunit, when *uncBEFH* DNA is cloned behind a strong promoter. Previous assembly models requiring α and β for formation of a functional F_0 may not be valid, and alternative interpretations of the observations leading to these models should be considered.

MATERIALS AND METHODS

Strains and plasmids. The *E. coli* strains constructed are listed in Table 1. P1 transduction with P1 *clr-100 cml*, and matings were performed as described by Miller (25). Transduction of *recA56* was done by the protocol of Mosher et al. (26). The 2-YT medium and LB medium used were those described by Miller (25). Competent cells were prepared and transformed by the procedure of Dagert and Ehrlich (3); transformants were selected on 2-YT agar plates supplemented with 50 to 100 μg of ampicillin per ml. The construction of plasmids is outlined in Fig. 1. Restriction enzyme digestions and ligations were done under the conditions recommended by the manufacturer (Bethesda Research Laboratories). Plasmids were routinely purified by the alkaline lysis procedure of Maniatis et al. (22) from a 5-ml culture of cells grown in 2-YT medium supplemented with 100 μg of ampicillin per ml.

IPTG induction of *unc* gene expression. Isopropyl-β-D-thiogalactoside (IPTG) was added to liquid medium or agar medium plates at 0.5 to 1 mM. In preliminary experiments with strain BP101 growing in LB medium with 50 μg of ampicillin per ml, IPTG was found to induce a transient lag in growth, after which growth continued to a normal stationary-phase density. When cells from this stationary culture

* Corresponding author.

TABLE 1. *E. coli* strains and plasmids

Strain or plasmid	Genotype or description	Source or reference
Strains		
JM83	*ara* Δ(*lac pro*) *rpsL thi* φ80 Δ*lacZM15*	(31)
JM103	Δ(*lac pro*) *thi rpsL endA sbcB15 hsdB15 hsdRF supE*, F′ (*traD36 proAB*$^+$ *lacI*^{q} *lacZM13*)	(23)
AN346	F′ *entA403 pyrE41 ilvC7 argH1 rpsL109*	(13)
MM180	*ilv*$^+$ *unc*$^+$ transductant of strain AN346	(26)
MM598	Strain MM180 lysogenized with λ cI857 *S7* and λ *asn-5* (*unc*$^+$) transducing phage	(8, 26)
CAG1688	*araD139* Δ(*ara leu*)*7697* Δ*lacX74 galU galK hsr hsm*$^+$ *rpsL*, F′ (*lacI*^{q} *lacZ*::Tn*5 proAB*$^+$)	C. Gross (Wisconsin) (1)
SG4044	F$^-$Δ(*gal blu*) *lac lon-100 proC*$^+$	(15)
CAG1128	F$^-$ *proC* Tn*10 leu thr lacY galK tonA thi supE*	C. Gross (Wisconsin)
DK3	Δ*unc*(*BEFHAGD*) *ilv*$^+$ *minA minB rpsL*	R. Simoni (Stanford) (20)
DK6	Δ*unc*(*BEFHAGDC*) *ilv*$^+$ *minA minB purE pdxC his met*	R. Simoni (Stanford) (21)
BP101	Strain JM103 transformed with plasmid pBP101	This study
BP102	Strain JM103 transformed with plasmid pBP102	This study
LW101	F′ *lacI*^{q} in Δ*uncB-D* background of AN346; *ilv*$^+$ succinate-minus transductant of strain AN346 with P1 lysate of DK3 (Δ*uncB-D*); mated with CAG1688 selecting Kan^r (Tn*5*) and *leu*$^+$	This study
LW105	Strain LW101 transformed with plasmid pBP101H, selecting for Amp^r	This study
LW107	Strain AN346 with *ilv*$^+$ *lon-100*; Tet^r *proC* cotranductant of strain MM180 with P1 lysate of strain CAG1128; resultant strain transduced with P1 lysate of strain sG4044 selecting for *pro*$^+$ and mucoid colony morphology	This study
LW108	Strain AN346 with *lon-100*; constructed as for strain LW107 with strain AN346 as recipient of P1 transduction from strain CAG1128	This study
LW111	F′ *lacI*^{q} of strain LW107; mating between CAG1688 and LW107, selecting Kan^r *leu*$^+$	This study
LW113	*ilv*$^+$, succinate-negative P1 transductant of LW108 by using P1 lysate from strain DK6 (*ilv*$^+$ Δ*uncB-C*)	This study
LW116	Strain LW111 transformed with plasmid pBP101, selecting for Amp^r	This study
LW125	F′ *lacI*^{q} *lon-100* Δ*uncB-C ilv*$^+$ derivative of strain AN346; strain LW113 mated with CAG1688 selecting for Kan^r *leu*$^+$	This study
LW128	Strain LW125 transformed with plasmid pBP101H, selecting for Amp^r	This study
Plasmids		
pUC9	(Fig. 1)	(24)
pRPG23	*Hin*dIII fragment containing *uncBEFHA*$^+$ ligated in plasmid pBR322 (Fig. 1)	(16)
pBP101	*Eco*RI fragment containing *uncBEFH*$^+$ genes of pRPG23 ligated in plasmid PUC9 (Fig. 1)	This study
pBP101H	Plasmid pBP101 treated with *Hin*dIII and religated to remove 60-base-pair *Hin*dIII fragment (Fig. 1)	This study
pBP102	*Eco*RI fragment containing *uncBEFH*$^+$ genes ligated in pUC9 in opposite orientation of pBP101 (Fig. 1)	This study

were tested for retention of the plasmid by plating on 2-YT plates supplemented with 100 μg of ampicillin per ml, only 1.7% of the cells were ampicillin resistant (Amp^r). To grow IPTG-induced cells with retention of the pBP101 plasmid, cultures were grown to a density of 0.4 to 0.8 units of absorbance at 550 nm in 2-YT medium supplemented with 100 μg of ampicillin per ml. Additional ampicillin was added to the exponentially growing cells to a final concentration of 400 μg/ml, and IPTG was added to a 1 mM final concentration. Cells were harvested from 30 to 90 min after the IPTG addition (Fig. 2). Under these conditions 100% of the cells retained the pBP101 plasmid for the duration of the IPTG treatment, as determined by plating on 2-YT–ampicillin medium.

Biochemical analysis. Membranes were prepared and stored in TMDG buffer (50 mM Tris hydrochloride [pH 7.5], 5 mM $MgCl_2$, 1 mM dithiothreitol, 10% [vol/vol] glycerol), and ATPase and protein were determined as described previously (27). One unit of ATPase activity equals 1 μmol of ATP hydrolyzed per min at pH 7.8 at 30°C with 0.4 mM ATP. Stripped membranes and a crude F_1 fraction were prepared (17), and the F_1-ATPase bound to the stripped membrane fraction was determined as described previously (27). Membranes were dissolved in sodium dodecyl sulfate, and proteins separated by electrophoresis on slab gels (20% acrylamide, 0.33% bisacrylamide) and silver stained as described by Hermolin et al. (17). The protocol used to measure ATP-dependent and NADH-dependent quenching of quinacrine fluorescence in HKM buffer (10 mM *N*-2-hydroxyethylpiperazine-*N*′-2-ethanesulfonate–NaOH [pH 7.5], NaOH, 0.3 M KCl, 5 mM $MgCl_2$) was as described previously (27). The rate of F_0-dependent H^+ translocation by membrane vesicles was measured by three methods. Osmotic shock membrane vesicles were prepared by the method of Kaback and co-workers and loaded with K^+-phosphate, and the H^+ influx in response to a valinomycin-generated membrane potential was measured with a pH electrode (6). Alternatively, inside-out membrane vesicles prepared with a French press were loaded with potassium by the method of Friedl et al. (9), and H^+ influx was measured after the addition of valinomycin. The adaptation of the Friedl et al. method (9) for indirectly measuring H^+ influx into inside-out membrane vesicles, via quenching of 9-amino-6-chloro-2-methoxyacridine fluorescence, in response to a valinomycin-induced K^+ diffusion potential was also employed (27).

RESULTS

Preliminary observations. In initial attempts to clone the 2.3-kilobase *Eco*RI fragment of pRPG23 into plasmid pUC9, we obtained 11 transformants of JM83 with plasmids carry-

ing *unc* inserts in orientation 2 and none with inserts in orientation 1 (Fig. 1). This result suggested that the *uncBEFH* genes may be lethal when cloned under the control of the *lac* promoter of pUC9. The cloning was attempted again, transforming strain JM103 rather than JM83, since in the JM103 host transcription from the *lac* promoter should be repressed due to overproduction of *lac* repressor by *lacI*^{q}. Of the strain JM103 transformants with the 2.3-kilobase *uncBEFH* insert, two contained a recombinant plasmid in orientation 1 (plasmid pBP101) and six contained a recombinant plasmid in orientation 2 (plasmid pBP102) (Fig. 1). Plasmid pBP101H is a derivative of plasmid pBP101 with the small *Hin*dIII fragment removed (Fig. 1).

Expression of *uncBEFH* genes inhibits growth. Strain BP101 (strain JM103 transformed by plasmid pBP101) did not form colonies on 2-YT–ampicillin media containing 0.5 to 1 mM IPTG, whereas colony formation by strain BP102 (strain JM103 transformed by plasmid pBP102) was not influenced by inclusion of IPTG in the 2-YT–ampicillin plates. When 5 mM *N,N*-dicyclohexylcarbodiimide (DCCD) was included in the 2-YT–ampicillin plates, a normal plating efficiency was observed with strain BP101. When IPTG was added to growing liquid cultures of strain BP101, growth ceased after approximately one generation time, whereas IPTG had no effect on the growth of strain BP102 (Fig. 2A). These results confirmed that expression of the *uncBEFH* genes, as controlled by IPTG induction, was deleterious to growth, perhaps as a consequence of an increase in H^+ permeability mediated by a functional, DCCD-sensitive F_0 sector.

Induction of *unc* genes in plasmid pBP101 causes an increase in F_0-mediated H^+ conductance. Membranes prepared from exponentially growing BP101 cells gave normal degrees

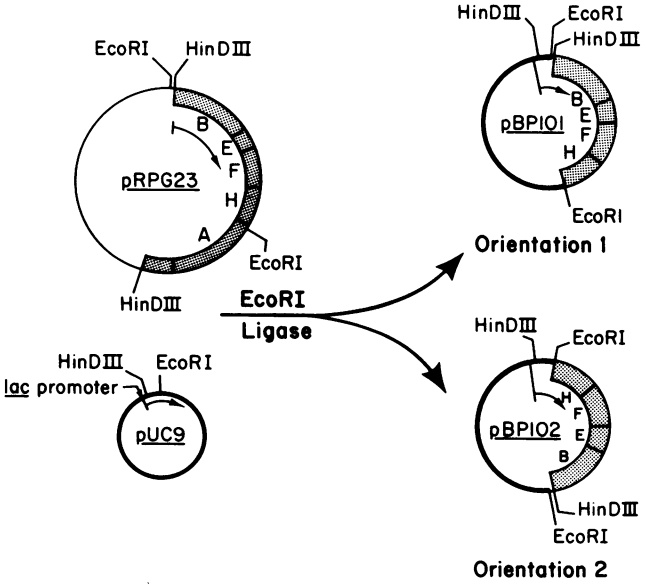

FIG. 1. Construction of plasmids pBP101 and pBP102. Plasmid pRPG23 was cleaved with *Eco*RI, and the digest was ligated with an *Eco*RI digest of plasmid pUC9. Plasmid pBP101H was generated from plasmid pBP101 by *Hin*dIII digestion and ligation with the exclusion of the 60-base-pair *Hin*dIII fragment. The direction of transcription from the *lac* promoter is indicated by the arrow. The size of the cloning region in pUC9 (*Hin*dIII → *Eco*RI) is exaggerated in the drawing.

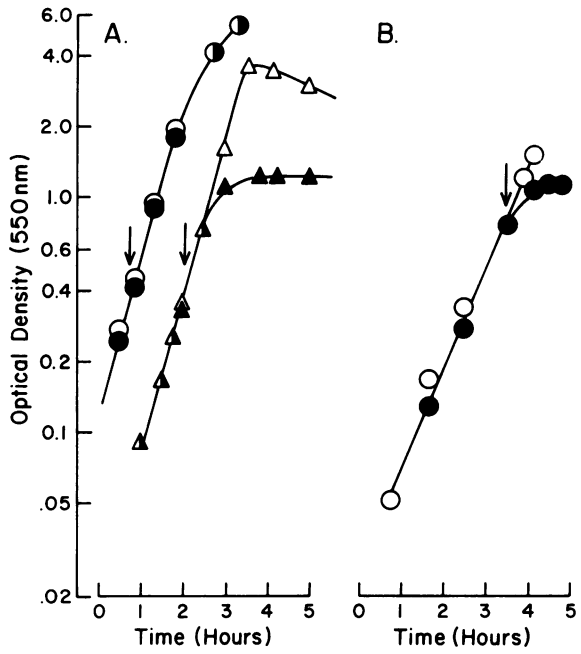

FIG. 2. Comparison of effects of IPTG on growth of strains transformed with plasmid pBP101 or pBP102. A, Strains BP101 (pBP101-transformed JM103) and BP102 (pBP102-transformed JM103) were grown in 1 liter of 2-YT medium containing 100 μg of ampicillin per ml in 4-liter flasks with gyratory shaking at 250 rpm. Growth was monitored with a Gilford spectrophotometer with appropriate dilution to ensure a linear accuracy of readings. Ampicillin and IPTG were added to 400 μg/ml and 1 mM, respectively, at the times indicated by the arrows. Growth was monitored to the stationary phase. Symbols: strain BP101 with (▲) and without (△) IPTG; strain BP102 with (●) and without (○) IPTG. B, Effect of IPTG on growth of strain LW105. Conditions are as in part A, with symbols indicating cultures monitored with (●) and without (○) IPTG addition.

of NADH- or ATP-dependent quenching of quinacrine fluorescence, but the magnitude of the quenching response was greatly reduced by IPTG-induced expression of the *unc* genes carried by the plasmid (Fig. 3; Table 2). Membranes prepared from noninduced, stationary-phase cells also gave a reduced quenching response (Fig. 3; Table 2). The latter effect was presumed to be due to the increase in cyclic AMP typically observed in stationary-phase cells (30) and the consequent reduction in the extent of catabolite repression. DCCD treatment of the membranes from IPTG-induced cells or noninduced, stationary-phase cells resulted in restoration of a normal quenching response (Table 2) and gave an additional indication that the abated fluorescence-quenching response was due to an increase in F_0-mediated H^+ conductance. The addition of F_1 to the H^+-leaky membranes partially restored the respiration-driven quenching response, adding greater weight to the suggestion that the reduced response was due to H^+ conductance mediated by a functional F_0.

Synthesis of a functional F_0 in the absence of F_1 subunits. The above results suggested that a functional F_0 could be synthesized in the absence of the coordinated synthesis of F_1 (5), in contrast to the prediction from the model of Cox et al. (2). However, it remained possible that F_1 subunits were required catalytically and were still mandatory in the synthesis of a functional F_0. To test this possibility, we con-

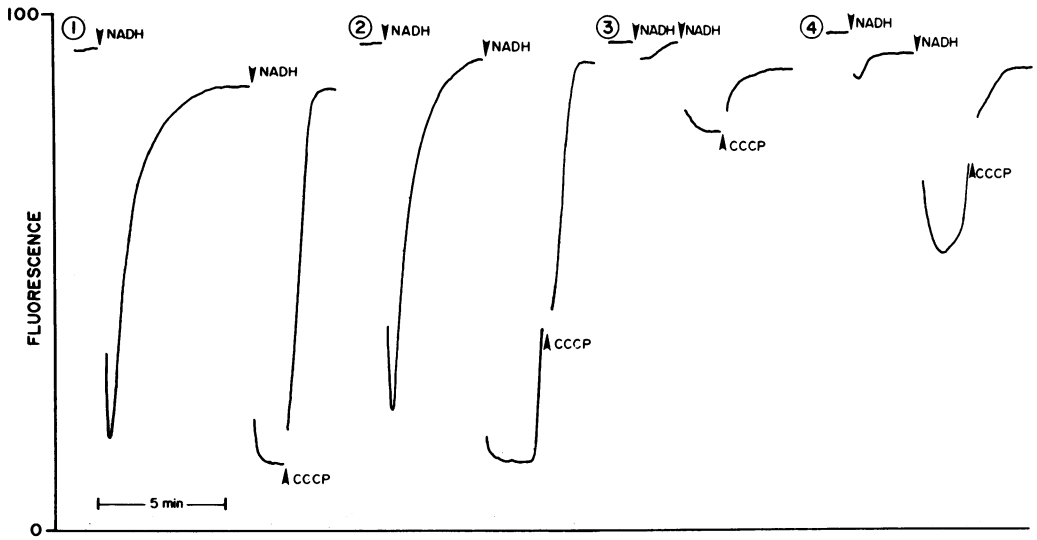

FIG. 3. NADH-dependent quenching of quinacrine fluorescence by BP101 and BP102 membranes. Membrane (550 μg of protein in 40 μl of TMDG buffer) was suspended in 1.0 ml of HKM buffer, and 5 μl of quinacrine (0.15 mg/ml) was added. At the times indicated, 5 μl of 10 mM NADH (first arrow), 10 μl of 100 mM NADH (second arrow), and 5 μl of 1 mM carbonyl cyanide *m*-chlorophenylhydrazone (CCCP) in ethanol were added, the tubes were mixed with a Vortex mixer, and the change in fluorescence (excitation, 450 nm; emission, 510 nm) was measured with an Aminco Bowman spectrofluorometer. Traces: 1, membrane from exponentially growing BP102 cells; 2, membrane from exponentially growing BP101 cells; 3, membrane from BP101 cells harvested 75 min after the addition of IPTG (Fig. 2A); 4, membrane of BP101 cells 90 min into the stationary phase.

structed strains containing a chromosomal deletion of the *uncBEFHAGD* or *uncBEFHAGDC* genes and *lacI*^{q} and transformed them with plasmid pBP101 or an indistinguishable derivative, plasmid pBP101H. In either of the *unc* deletion backgrounds, IPTG induction of plasmid pBP101 or pBP101H increased the DCCD-sensitive H^+ conductance of the membrane as judged from the degree of NADH-dependent quenching of quinacrine fluorescence (Table 2; data not shown). The quenching response was again partially restored by binding of F_1 to the membranes.

In the strain AN346 Δ*unc* background, with the F′ *lacI*^{q} episome used, a less dramatic inhibition of growth was observed on IPTG induction of the pBP101 plasmid than in the JM103 (*unc*$^+$) background (Fig. 2B). The more marginal inhibition of growth was also apparent in plating experiments where distinct but smaller colonies of strain LW105 were observed on 2-YT plates supplemented with ampicillin and IPTG versus medium lacking IPTG.

Degree of expression of functional F_0 by pBP101 plasmids in *unc* deletion strains. The three subunits of F_0, coded by the *uncBEF* genes on the pBP101 or pBP101H plasmid, were synthesized in sufficient quantity to be observed in the crude membrane fraction of IPTG-induced cells (Fig. 4, lane 2). The ψ subunit is not well resolved from the bands of two constitutive membrane proteins seen in strain LW101 (Δ*uncB-D*), but the increase in staining of a band above these bands is apparent. The band corresponding to ψ was more apparent on visual examination of the silver-stained gel, since the three bands are different colors. Exact quantitation of the extent of F_0 subunit incorporation in the membrane is complicated by bands neighboring ψ and χ in this gel and a series of other sodium dodecyl sulfate-acrylamide gels that were run. We estimate that the amount of F_0 incorporated in the IPTG-induced LW105 membranes shown is approximately two to three times the monoploid level, based upon comparison to the induced λ-*unc*$^+$ membranes with F_1F_0

TABLE 2. Effect of induction of pBP101 on ATP- and NADH-dependent quenching of quinacrine fluorescence with membranes *unc*$^+$ and Δ*unc* strains

Strain	Growth phase or conditions	% Quenching[a]					
		ATP	50 μM NADH[b]			1 mM NADH	
			Control	DCCD	F_1	Control	DCCD	F_1
BP102[c]	Exponential	77	80	86		85	86	
BP101	Exponential (uninduced)	77	79	83		83	85	
BP101	IPTG, 30 min	16	5	78	39	20	87	59
BP101	IPTG, 75 min	8	3	68	16	18	87	45
BP101	Stationary	45	8	76	25	39	90	80
LW101	Exponential	<3	79	81		83	82	
LW105	Exponential (uninduced)	<3	69	80	66	81	82	80
LW105	IPTG, 60 min	<1	9	74	21	48	87	71

[a] NADH response indicated after no treatment (control), incubation of membranes with 20 μM DCCD for 20 min, and incubation of membranes with 1 unit of F_1 per 0.55 mg of membrane protein for 5 min before dilution into assay buffer.
[b] The initial rate of oxidation of 50 μM NADH is approximately 50% of the rate observed with 1 mM NADH.
[c] The response shown by BP102 membranes was equivalent to that given by JM103 membranes.

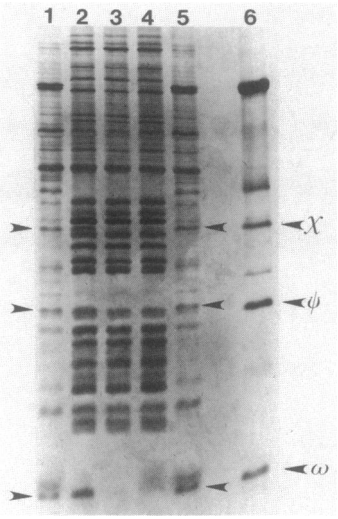

FIG. 4. Analysis of pBP101-induced F_0 subunit production in crude membrane fraction by sodium dodecyl sulfate-gel electrophoresis and silver staining. Lanes: 1 and 5, control membranes (1.5 μg of protein) from heat-induced (λ-*unc*$^+$) strain MM598; 2, 2 μg of membrane protein from IPTG-induced strain LW105 (pBP101H in Δ*uncB-D*); 3, 2 μg of membrane protein from uninduced, exponentially growing strain LW105; 4, 2 μg of membrane protein from strain LW101 (Δ*unc*B-D); 6, F_1F_0 standard. Horizontal arrows indicate the positions of the subunits.

present at approximately six times that of monoploid *unc*$^+$ strains (8) (Fig. 4, lanes 1 and 5) and to strain JM103 (data not shown). Somewhat greater incorporation has been observed in strain BP101 with more prolonged induction times, e.g., up to six times the monoploid level after 75 to 150 min of IPTG treatment. The ratio of subunits incorporated did not differ dramatically from the wild type, although as much as a twofold excess of ω relative to χ was apparent in most gels. The staining intensity of ψ relative to χ was also reduced in some gels, e.g., by 30 to 40% in the gel shown (Fig. 4, lane 2).

The magnitude of F_0 formation is also indicated by the amount of F_1 bound to membranes of *unc* deletion strains in which the plasmid-coded F_0 genes were induced (Fig. 5). The amount of F_1 bound to induced LW128 or LW105 membranes was 1.3 to 2.0 times that of unstripped monoploid *unc*$^+$ membranes (Fig. 5A). The specific activity of stripped membranes reconstituted with F_1 was higher (Fig. 5B) due to removal of other extrinsic membrane proteins. In the case of strain LW128, stripped membranes bound 1.2 times the amount of F_1 bound by wild-type stripped membrane.

We attempted to quantitatively compare F_0-mediated H^+ conductance of membranes prepared from strains in which the pBP101 plasmid was induced versus membranes prepared from strains lacking the plasmid. Induction of F_0 expression from the plasmid in strain LW128 resulted in a 5- to 10-fold increase in H^+ permeability over that observed in the *unc* deletion strain LW125, i.e., to a level of H^+ permeability approximately that of monoploid, wild-type stripped membranes (strain MM180 in Fig. 6A and Table 3). An increase in H^+ permeability of similar magnitude was observed on comparing LW101 (Δ*unc*) and induced LW105 (pBP101H, Δ*unc*) membranes by measuring the rate of 9-amino-6-chloro-2-methoxyacridine quenching after imposition of a K^+ diffusion potential (Table 3) and measuring H^+ influx into Kaback-type vesicles with a pH electrode (Fig. 6B; Table 3). The magnitude of the increase in H^+ conductance was approximately that expected from the observed degree of subunit overproduction (Fig. 4) and F_1 binding (Fig. 5).

Role of protein degradation in synthesis of partially functional F_0. The synthesis of F_0 directed from plasmid pBP101 invariably resulted in an H^+-leaky membrane that was not completely sealed by binding of F_1 (Table 2). One possible explanation stems from the susceptibility of the ψ subunit to proteolysis when F_1 is not bound (17, 18, 29). We constructed a series of strains in an *lon* backgound, since the *lon* locus seems to be important in intracellular protein degradation in *E. coli* (15). Membranes prepared from cells in which F_0 synthesis was induced in an *lon-100* background gave only a marginally greater restoration of NADH- or ATP-driven quenching, after the binding of F_1, relative to those from an *lon*$^+$ background (Fig. 7).

DISCUSSION

We have demonstrated that a functional F_0 can be assembled in the absence of synthesis of the α, β, γ and ε subunits of F_1. Previously, two laboratories had proposed that the α and β subunits of F_1 played an important role either in the integration of the ψ subunit into the membrane or in the assembly of a functional F_0 (2, 20). One of the major questions we have attempted to address is whether the F_0 that integrates in the membrane in the absence of α and β subunits is fully functional. We did find a reasonable correlation between the amount of F_0 inserted and F_0 function. With the *unc* deletion strains, the ψ and χ subunits of F_0 were found at approximately two to three times the monoploid level after limited periods of induction. F_0-mediated H^+ conduction and F_1 binding were measured at a level one to two times that of monoploid membranes. We would therefore estimate that the F_0 formed under these conditions must be at least 33 to 50% as active as that of native membranes.

We were not able to completely restore the maximal ATP-dependent quenching response on binding of F_1 to membranes from the induced *unc* deletion strains. One possible explanation is a partial proteolysis of the ψ subunit. Previous reports indicate that when the ψ subunit of stripped

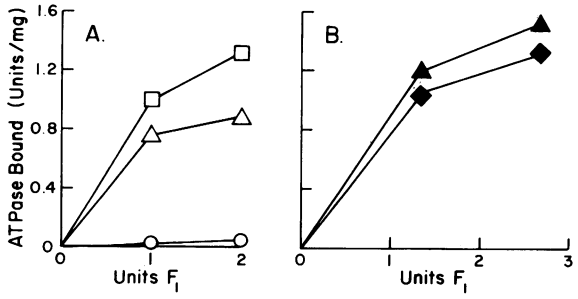

FIG. 5. Binding of F_1 to native or stripped membranes after IPTG induction of F_0 synthesis from plasmid pBP101H. A, F_1 binding to native membrane of strain LW101 (Δ*uncB-D*) (○) or native membranes from IPTG-induced strains LW105 (pBP101H, Δ*uncB-D*) (□), and LW128 (pBP101H, Δ*uncB-C*, *lon*) (△). B, Comparison of F_1 binding to stripped membranes of monoploid *unc*$^+$ strain MM180 (◆) with that by stripped membrane from IPTG-induced strain LW128 (▲). F_1 was incubated with 1 mg of membrane protein in 2 ml of TMDG buffer, and the activity bound to the membrane was determined after centrifugation and washing.

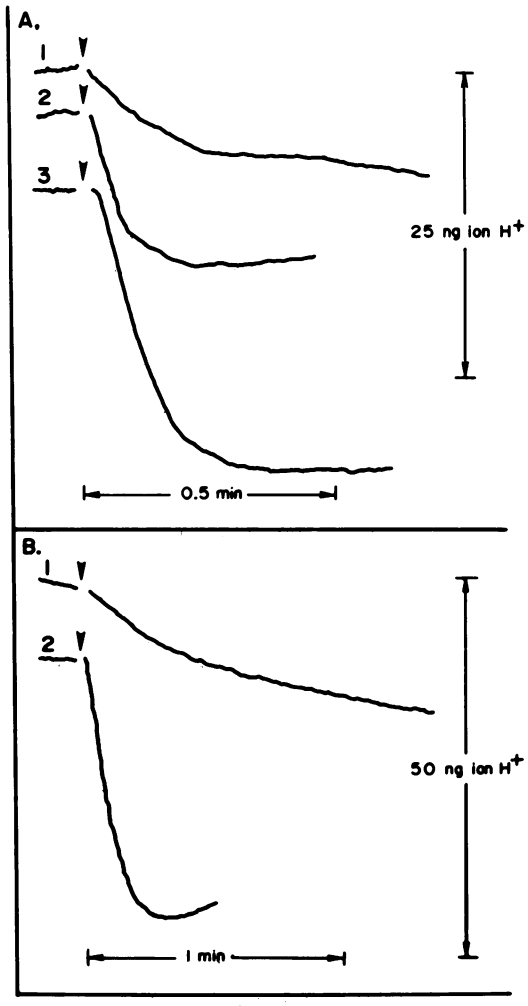

FIG. 6. Valinomycin-stimulated H^+ influx into K^+-loaded membrane vesicles as measured with a pH electrode. A, Vesicles prepared with a French press. Traces: 1, strain LW125 (*ΔuncB-C, lon*); 2, stripped membranes of strain MM180 (*unc*$^+$); 3, IPTG-induced strain LW128 (pBP101H, *ΔuncB-C, lon*). B, Vesicles prepared by osmotic shock. Traces: 1, strain LW101 (*ΔuncB-D*); 2, IPTG-induced strain LW105 (pBP101H, *Δunc*B-D). Valinomycin was added where indicated by the arrows.

membranes is degraded, F_1 binding function is lost without diminishing F_0-mediated H^+ conductance (17, 29). Hoppe et al. (18) have reported that such degradation normally takes place in stationary-phase cells lacking F_1. We did estimate a slight reduction in the ψ/χ ratio in membranes from induced *unc* deletion strains, but we should emphasize the inherent uncertainty in such estimates. The preferential proteolysis of ψ relative to χ would result in membranes with the properties described, i.e., an F_0 H^+ conductor that was completely blocked by DCCD but only partially blocked by the binding of F_1. Results similar to those given in Fig. 7B would be obtained with wild-type membranes depleted of one-third the monoploid level of bound F_1 (27). With overproduction, the fractional deficit in the ψ/χ ratio necessary to cause an H^+ leak of the magnitude measured would be less than the one-third.

A question we cannot answer is whether the rate of insertion of F_0 into the membrane is optimal in the absence of α and β subunit production. In the system we have used, the F_0 genes are cloned on a multicopy plasmid behind a strong promoter, and one might expect to see greater overproduction of F_0 than that observed. In strain BP101, F_0 production does appear to plateau at approximately six times the monoploid level after 60 to 90 min of IPTG treatment, and we chose not to extend the induction because the cells enter the stationary phase. The extent of F_0 production in *unc* deletion strains is definitely smaller during a 60-min induction period. The difference could be due to the complete absence of α and β and a requirement for these subunits in enhancing the rate of insertion. Alternatively, the physiological conditions imposed by the *unc* phenotype may reduce F_0 synthesis and insertion. Growth is slower, and the number of ribosomes and perhaps the plasmid copy number may be lower.

The conclusions reported here differ from those of Klionsky et al. (20), who cloned the same *Eco*RI fragment of plasmid pRPG23 into the chloramphenicol resistance gene of plasmid pACYC184, generating plasmid pRPG45. Synthesis of radioactive subunits corresponding to χ, ω, and ψ was observed in the membrane of minicells, but the cellular membrane was judged to be proton impermeable and the F_0 was judged to be nonfunctional after the addition of F_1. One possible explanation for the discrepancy is the strength of the promoter behind which the genes were cloned. There may have been sufficient expression to detect F_0 synthesis with radioactive tracers in minicells, but insufficient expression to detect function. Transformation with additional plasmids coding the five subunits of F_1 did result in a small ATP-dependent fluorescence quenching response, but the quenching response with 0.5 mM NADH remained insensitive to the stripping of F_1 from the membrane. The incomplete restoration of function may be consistent with a very low level of F_0 expression from pRPG45. A low level of F_0-mediated H^+ conductance might more readily be detected by use of lower concentrations of NADH (Table 2) (27).

Aris et al. have recently reexamined the issue of whether

TABLE 3. Comparison of initial rates of H^+ influx into membrane vesicles[a]

Strain	Initial rate of H^+ influx (nmol of H^+/s)		Rate of ACMA quenching[b]
	French press vesicles[c]	Osmotic shock vesicles[d]	
Δunc control			
Strain LW101		0.3 ± 0.1 (3)	0.6 ± 0.7 (3)
Strain LW125 (*lon*)	0.6 ± 0.1 (4)		
Δunc with induced pBP101			
Strain LW105		6.1 ± 0.7 (2)	4.3 ± 1.6 (3)
Strain LW128 (*lon*)	4.2 ± 1.6 (6)		
Stripped *unc*$^+$			
Strain MM180	5.4 ± 2.7 (4)		3.1 ± 1.4 (4)

[a] Membrane vesicles were loaded with K^+, and the initial rate of H^+ influx or fluorescence quenching was determined after the addition of valinomycin to generate a K^+ diffusion potential. Values given are average ± standard deviation, with the number of determinations within parentheses.

[b] Measurement with 2 mg of protein per 3.2 ml. Expressed as the percentage of the initial fluorescence quenched per second. ACMA, 9-Amino-6-chloro-2-methoxyacridine.

[c] Measured with 3.3 mg of protein per ml. Average of two independent experiments.

[d] Measurement with 4 mg of protein per 2.5 ml.

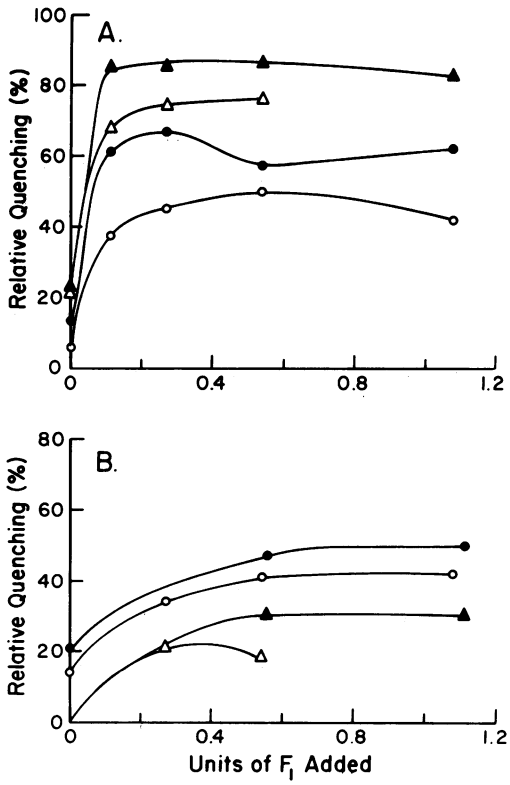

FIG. 7. Partial restoration of NADH-dependent and ATP-dependent quinacrine quenching response to H^+-permeable membranes by binding of F_1, comparing *lon-100* and *lon*$^+$ backgrounds. Membranes (300 μg of protein) were incubated at room temperature with the units of F_1 ATPase indicated for 5 min in HKM buffer or with 20 μM DCCD in HKM buffer for 20 min. A, Comparison of IPTG-induced *unc*$^+$ strains BP101 (△, ○) and LW116 (*lon-100*) (▲, ●). The quenching response given by 50 μM NADH (△, ▲) or 1 mM ATP (○, ●) is normalized to the extent of quenching by 50 μM NADH after DCCD treatment (100% relative quenching). B, Comparison of IPTG-induced Δ*unc* strains LW105 (△, ○) and LW128 (*lon-100*) (▲, ●). Symbols for NADH and ATP are as in part A.

a functional F_0 is formed from plasmid pRPG45, and related plasmids carrying the F_0 genes, in strains lacking F_1 subunits (1a). They conclude that F_1 subunits are not required for assembly of a functional F_0 and suggest that the previously described difference in F_0 function, seen on comparing strains with and without F_1 subunits, may have been due to F_1 subunits protecting F_0 from proteolysis.

The apparent discrepancy between this work and the model of Cox et al. (2) is more difficult to rationalize. The proposed model provides a simple and elegant explanation for the observations made. An argument could be made that α and β kinetically promote insertion of the ψ subunit of F_0 under normal in vivo conditions and that overexpression of F_0 subunits from the pBP101 plasmid thermodynamically forces F_0 insertion in our system. However, alternative interpretations of the experimental results of Cox et al. (2) should also be considered. One question relates to the sensitivity of the two-dimensional gels used to detect subunit ψ. The F_1-binding results reported previously (2) might suggest that at least some ψ subunit was incorporated in the membrane. It also seems possible that some ψ was incorporated and then degraded as suggested by Friedl et al. (10). Incorporation of ψ with other F_0 subunits, even if in a degraded form, should lead to an H^+-permeable membrane, and this was not detected by the quenching studies with NADH. However, as we have stressed here and elsewhere (27), this assay can be relatively insensitive when done with high concentrations of NADH that promote maximal rates of oxidation. The level of incorporation of the χ and ω subunits was either not determined or not quantitatively reported for the mutants examined by Cox et al. (2), and the amount of F_0 function expected cannot be ascertained. It would also be useful to have this information in interpreting the specificity of the effect. Since the Cox et al. report, strains with mutations in both *uncH* (19, 28) and *uncC* (21) have been reported with phenotypes similar to the *uncA* and *uncD* mutants described previously (2). That is, the mutant membranes lack F_1 but are proton impermeable as judged by the NADH quenching response. These results may indicate that a more general regulatory process coordinates F_0 and F_1 formation.

ACKNOWLEDGMENTS

We thank R. Simoni and D. Klionsky for the *unc* deletion strains used in these studies, R. Gunsalus for plasmid pRPG23, and C. Gross for other strains indicated in Table 1.

This work was supported by Public Health Service grant GM-23105 from the National Institutes of Health.

LITERATURE CITED

1. **Casadaban, M. J., and S. N. Cohen.** 1980. Analysis of gene control signals by DNA fusion and cloning in *Escherichia coli*. J. Mol. Biol. **138**:179–207.

1a. **Aris, J., D. J. Klionsky, and R. D. Simoni.** 1985. The F_0 subunits of the *Escherichia coli* F_1F_0-ATP synthase are sufficient to form a functional proton pore. J. Biol. Chem. **260**:11207–11215.

2. **Cox, G. B., J. A. Downie, L. Langman, A. E. Senior, G. Ash, D. R. H. Fayle, and F. Gibson.** 1981. Assembly of the adenosine triphosphatase complex in *Escherichia coli*: assembly of F_0 is dependent on the formation of specific F_1 subunits. J. Bacteriol. **148**:30–42.

3. **Dagert, M., and S. D. Ehrlich.** 1979. Prolonged incubation in calcium chloride improves the competence of *Escherichia coli* cells. Gene **6**:23–28.

4. **Fillingame, R. H.** 1981. Biochemistry and genetics of bacterial H^+-translocating ATPases. Curr. Top. Bioenerg. **11**:35–106.

5. **Fillingame, R. H.** 1984. F_0 sector of *E. coli* ATP synthase, p. 109–118. *In* S. Papa, K. Altendorf, L. Ernster, and L. Packer (ed.), H^+-ATPase (ATP synthase): structure, function, regulation. ICSU Press by Adriatica Editrice, Bari, Italy.

6. **Fillingame, R. H., K. Knoebel, and A. E. Wopat.** 1978. Method for isolation of *Escherichia coli* mutants with defects in proton-translocating sector of the membrane adenosine triphosphatase complex. J. Bacteriol. **136**:570–581.

7. **Foster, D. L., and R. H. Fillingame.** 1982. Stoichiometry of subunits in the H^+-ATPase complex of *Escherichia coli*. J. Biol. Chem. **257**:2009–2015.

8. **Foster, D. L., M. E. Mosher, M. Futai, and R. H. Fillingame.** 1980. Subunits of the H^+-ATPase of *Escherichia coli*: overproduction of an eight-subunit F_1F_0-ATPase following induction of a λ-transducing phage carrying the *unc* operon. J. Biol. Chem. **255**:12037–12041.

9. **Friedl, P., G. Bienhaus, J. Hoppe, and H. U. Schairer.** 1981. The dicyclohexylcarbodiimide binding protein *c* of ATP synthase from *Escherichia coli* is not sufficient to express an efficient H^+-conduction. Proc. Natl. Acad. Sci. USA **78**:6643–6646.

10. **Friedl, P., J. Hoppe, R. P. Gunsalus, O. Michelsen, K. von Meyenburg, and H. U. Schairer.** 1983. Membrane integration and function of the three F_0 subunits of the ATP synthase of *Escherichia coli* K12. EMBO J. **2**:99–103.

11. **Futai, M., and H. Kanazawa.** 1983. Structure and function of proton-translocating adenosine triphosphatase (F_0F_1): biochemical and molecular biological approaches. Microbiol. Rev. **47**:285–312.

12. **Gay, N. J.** 1984. Construction and characterization of an *Escherichia coli* strain with a *uncI* mutation. J. Bacteriol. **158**:820–825.
13. **Gibson, F., G. B. Cox, J. A. Downie, and J. Radik.** 1977. Partial diploids of *Escherichia coli* carrying normal and mutant alleles affecting oxidative phosphorylation. Biochem. J. **162**:665–670.
14. **Gibson, F., J. A. Downie, G. B. Cox, and J. Radik.** 1978. Mu-induced polarity in the *unc* operon of *Escherichia coli*. J. Bacteriol. **134**:728–736.
15. **Gottesman, S., and D. Zipser.** 1978. Deg phenotype of *Escherichia coli lon* mutants. J. Bacteriol. **133**:844–851.
16. **Gunsalus, R. P., W. S. A. Brusilow, and R. D. Simoni.** 1982. Gene order and gene-polypeptide relationships of the proton-translocating ATPase operon (*unc*) of *Escherichia coli*. Proc. Natl. Acad. Sci. USA **79**:320–324.
17. **Hermolin, J., J. Gallant, and R. H. Fillingame.** 1983. Topology, organization and function of the psi subunit in the F_0 sector of the H^+-ATPase of *Escherichia coli*. J. Biol. Chem. **258**:14550–14555.
18. **Hoppe, J., P. Friedl, H. U. Schairer, W. Sebald, K. von Meyenburg, and B. B. Jorgensen.** 1983. The topology of the proton translocating F_0 component of the ATP synthase from *E. coli* K12: studies with proteases. EMBO J. **2**:105–110.
19. **Humbert, R., W. S. A. Brusilow, R. P. Gunsalus, D. J. Klionsky, and R. D. Simoni.** 1983. *Escherichia coli* mutants defective in the *uncH* gene. J. Bacteriol. **153**:416–422.
20. **Klionsky, D. J., W. S. A. Brusilow, and R. D. Simoni.** 1983. Assembly of a functional F_0 of the proton-translocating ATPase of *Escherichia coli*. J. Biol. Chem. **258**:10136–10143.
21. **Klionsky, D. J., W. S. A. Brusilow, and R. D. Simoni.** 1984. In vivo evidence for the role of the ε subunit as an inhibitor of the proton-translocating ATPase of *Escherichia coli*. J. Bacteriol. **160**:1055–1060.
22. **Maniatis, T., E. F. Fritsch, and J. Sambrook.** 1982. Molecular cloning: a laboratory manual. Cold Spring Harbor Laboratory, Cold Spring Harbor, N.Y.
23. **Messing, J., R. Crea, and P. H. Seeburg.** 1981. A system for shotgun DNA sequencing. Nucleic Acids Res. **9**:309–321.
24. **Messing, J., and J. Vieira.** 1982. A new pair of M13 vectors for selecting either DNA strand of double-digest restriction fragments. Gene **19**:269–276.
25. **Miller, J. H.** 1972. Experiments in molecular genetics. Cold Spring Harbor Laboratory, Cold Spring Harbor, N.Y.
26. **Mosher, M. E., L. K. Peters, and R. H. Fillingame.** 1983. Use of lambda *unc* transducing bacteriophages in genetic and biochemical characterization of H^+-ATPase mutants of *Escherichia coli*. J. Bacteriol. **156**:1078–1092.
27. **Mosher, M. E., L. K. White, J. Hermolin, and R. H. Fillingame.** 1985. H^+-ATPase of *Escherichia coli*: an *uncE* mutation impairing coupling between F_1 and F_0 but not F_0-mediated H^+-translocation. J. Biol. Chem. **260**:4807–4814.
28. **Noumi, T., and H. Kanazawa.** 1983. Mutants of *Escherichia coli* H^+-ATPase defective in the δ subunit of F_1 and the b subunit of F_0. Biochem. Biophys. Res. Commun. **111**:143–149.
29. **Perlin, D. S., D. N. Cox, and A. E. Senior.** 1983. Integration of F_1 and the membrane sector of the proton-ATPase of *Escherichia coli*: role of subunit "b" (*uncF* protein). J. Biol. Chem. **258**:9793–9800.
30. **Peterkofsky, A.** 1976. Cyclic nucleotides in bacteria. Adv. Cyclic Nucleotide Res. **7**:1–48.
31. **Vieira, J., and J. Messing.** 1982. The pUC plasmids, an M13 mp7-derived system for insertion mutagenesis and sequencing universal primers. Gene **19**:259–268.
32. **Walker, J. E., M. Saraste, and N. J. Gay.** 1984. The *unc* operon: nucleotide sequence, regulation and structure of ATP-synthase. Biochim. Biophys. Acta **768**:164–200.